Planning Active Distribution Networks Considering Multi-DG Configurations

Sultan S. Al Kaabi, *Member, IEEE*, H. H. Zeineldin, *Senior Member, IEEE*, and Vinod Khadkikar, *Member, IEEE*

***Abstract*—Planning distribution systems without considering the operation status of multiple distributed generation (DG) units could result in constraining the network, lowering the utilization of its assets and minimizing the total DG capacity that can be accommodated. In this paper, the impact of multiple DG configurations on the potential of active network management (ANM) schemes is firstly investigated. Secondly, the paper proposes a multi-configuration multi-period optimal power flow (OPF)-based technique (MMOPF) for assessing the maximum DG capacity under ANM schemes considering 1) variability of demand and generation profiles (multi-period scenarios), and 2) different operational status of DG units (multi-configurations). The results show that the availability of DGs at certain locations could critically impact the amount of DG capacity at other locations. If DGs are properly allocated and sized at certain locations up to the optimal limits, even with a "fit-and-forget" approach, the total connected DG capacity can be maximized, with minimum utilization of ANM schemes. However, exceeding these optimal limits may lead to minimizing the total DG penetration in the long term, impacting the system reliability due to the operational status of multiple DG units, and consequently, imposing more investments on ANM schemes to increase the amount of connected DG capacity.**

***Index Terms*—Active network management, distributed generation, optimal power flow, power distribution planning.**

NOMENCLATURE

i, j, N	Indices of ith and jth bus; for a total of N buses in the system, $(i, j \in N)$.
DG_N	Total number of DG units in the system.
m, M	Index of mth multi-period scenario; for a total of M multi-period scenarios, $(m \in M)$.
α_m, γ_m	Levels of DG generation and demand profiles for mth multi-period scenario.
c, MC_N	Index of cth multi-configuration; for total a of MC_N multi-configurations, $(c \in MC_N)$.
β_i^c, β	Operational status of individual DG unit; and all DG units at ith bus and cth configuration.
$P_{i,m}^c$, $Q_{i,m}^c$	Nodal active and reactive power injection.
$P_{G_{i,m}}^c$, $Q_{G_{i,m}}^c$	Active and reactive grid generation.
P_{D_i}, Q_{D_i}	Active and reactive demand.
$V_{i,m}^c$, $\delta_{i,m}^c$	Voltage magnitude and angle.
$T_{t,m}^c$, t, TR_N	Tap setting of tth OLTC transformer; for a total of TR_N OLTC transformers, $(t \in TR_N)$.
$\theta_{i,m}^c$	DG power angle.
$P_{DG_{i,m}}^c$, $Q_{DG_{i,m}}^c$	DG active and reactive powers.
$P_{i,j,m}^c$, $Q_{i,j,m}^c$	Active and reactive power flows in the line connecting ith and jth buses, $(i, j \in N)$.
$S_{ij}^{\max}$	Thermal limit (in MVA).
R, X	Line resistance and reactance.
G_{ij}, B_{ij}	ijth element of the Y-bus matrix.
bc_{ij}	Shunt capacitance of the line.
$P_{DG_i}^c$	Maximum DG capacity of new DG unit at$i$th bus and cth configuration.
$P_{DG_i}^{opt}$, P_{DG}^{opt}	Optimal DG capacity of a DG unit at ith bus; and total DG capacity of all DG units.
$DG^{\max}$	Upper bound on the DG capacity.

Manuscript received March 17, 2013; revised June 22, 2013 and August 05, 2013; accepted September 09, 2013. This work was supported in part by the Masdar Institute of Science and Technology and in part by the Abu Dhabi Water and Electricity Authority (ADWEA). Paper no. TPWRS-00325-2013.

S. S. Al Kaabi and V. Khadkikar are with the Institute Centre for Energy, Electrical Engineering and Computer Science Department, Masdar Institute of Science and Technology, Abu Dhabi, United Arab Emirates (e-mail: salkaabi@masdar.ac.ae; vkhadkikar@masdar.ac.ae).

H. H. Zeineldin was with the Faculty of Engineering, Cairo University, Giza, Egypt, and is now with the Institute Centre for Energy, Electrical Engineering and Computer Science Department, Masdar Institute of Science and Technology, Abu Dhabi, United Arab Emirates (e-mail: hzainaldin@masdar.ac.ae).

Digital Object Identifier 10.1109/TPWRS.2013.2282343

I. INTRODUCTION

THE typical investment plan to meet future demand growth and its associated infrastructures could be deferred by introducing distributed generations (DGs) in transmission or distribution networks [1]. The presence of DGs in distribution networks could improve the system efficiency, reliability, security and quality of service [2], [3]. However, they could critically impact the system voltage, power quality and stability, fault level and interact with the operation of capacitors, voltage regulators and protection coordination [4]–[7]. The intermittency and variability of renewable-type DGs (e.g., wind and PV) impose challenges when planning distribution systems [8]–[13].

Under a passive network scheme, DGs are usually operated with fixed power factor(s) and on-load-tap-changers (OLTCs) are restricted to only regulate the secondary voltages [14]–[18]. Distribution and transmission system operators

(DSOs and TSOs) traditionally install firm-DGs based on the "fit-and-forget" approach, while generation curtailment of multiple DG units with non-firm connections is applied based on the "last-in-first-out" approach [18]–[24].

In the last decade, the emerging active network management (ANM) schemes have proved to be beneficial for DSOs and TSOs, compared to passive network management [14]. ANM schemes can enhance and maximize the utilization of network's assets, which could allow the existing distribution networks to accommodate more DG capacity under the current infrastructure and hence, defer or avoid costly network upgrades. The major ANM schemes include coordinated voltage control (CVC) of OLTCs and voltage regulators, compensator reactive power control, DG's power factor control (PFC) and energy curtailment (EC) [14]–[18]. Also, optimal generation curtailment scheme of ANM is beneficial to mitigate voltage problems as compared to the "last-in-first-out" approach [19]–[24].

Recently, many research studies have been reported on ANM highlighting the benefits, introducing new schemes and applications. Some studies demonstrated practical projects, implementations, and experiences of ANM [25]–[27], online ANM application [28], [29], combined ANM with demand response application [30] and ANM challenges for networks' operators [31]. In [32]–[35], the techno-economic assessment and cost-benefit analysis of investments and operation costs for various combinations of ANM schemes are studied and compared against passive network management scheme. In general, it is found that as the DG penetration increases the investment costs of ANM schemes become more viable and justifiable.

Nowadays, due to the increasing trend toward integrating more DGs in transmission and distribution networks, the planning scope of maximizing DG penetration is taking the priority of DSOs and TSOs in most countries. However, the steady-state voltage rise is one of the main network constraints which limit the amount of DG capacity that can be accommodated [36]. In [37], the voltage problem associated with the random installation of customer owned DGs, in terms of location, type and size, is examined on a secondary distribution network. In [38], the proposed method incorporates voltage step change constraint to cater for the impact associated with sudden disconnection or connection of a DG. The results show significant reduction in the amount of DG capacity when voltage step constraint is applied, and a wider step constraint could result in higher DG capacity.

Some ANM studies, analyzed the potential of ANM schemes to maximize DG penetration [15], [16], maximize energy exploitation [17] and minimize energy losses [18]. The impact of variable demand and generation profiles is also investigated with multi-period optimal power flow (OPF)-based (MOPF) technique [16]–[18]. These studies are tested under "fixed" DG locations with only one DG-configuration (all DGs operating), and it was found that: 1) ANM potential is limited when OLTC's are restricted in mitigating voltage rise, and 2) certain DG locations are not affected by integrating extra ANM schemes due to reaching thermal line limit with little utilization of ANM, while other DG locations are considerably affected when more ANM schemes are utilized. However, the impacts of multi-DG configurations are not considered in [15]–[18], which could critically affect the potential of ANM schemes and the amount of connected DG capacity. Here the term multi DG-configurations refers to the operational status of DG units (ON or OFF) in the network.

The relationship between maximizing DG capacity and steady-state voltage violation is investigated using a voltage sensitivity factor in [39] and [40]. In [40], an effective method is proposed that allocates DGs based on analyzing various constraints associated with each bus to ensure no network sterilization occurs. Network sterilization results when DG units are allocated individually rather than a group at certain locations which can result in constraining the network, minimizing the total connected DG capacity and lowering the utilization of existing assets. In [41], another method is proposed that identifies strong and weak buses, and then, places DGs at buses with strong voltage stability margins. In [42], the effect of selecting various DG penetration targets is found to result in different DG allocations. As the target incrementally increased, the results show considerable increase or decrease in DG capacity at certain locations. Hence, the evaluation of total DG penetration based on all locations is found to be optimal for the long term planning. All these studies [39]–[42] showed that small DG penetration at certain locations could cause severe voltage problems, and hence, affect the total DG penetration. However, these studies also did not consider the effect of multi DG-configurations which could considerably impact the allocations and amount of connected DG capacity.

Generally, conventional planning studies involving DG integration do not consider the dynamic nature of the power system operation [15]–[18], [39]–[42]. For example, these planning studies do not address the impact on the overall DG penetration level when one or more existing DG units are absent, which are possible scenarios in the operational stage. Therefore, the major contributions of this paper are highlighted as follows:

1) Provides detailed analysis and results on how multi-DG interactions could impact the amount of connected DG capacity as well as the utilization of ANM schemes.
2) Proposes a new OPF-based planning approach which takes into account the operational status of DG units at the planning stage, and evaluates the DG capacity considering various multi-DG configurations which has not been addressed so far.

II. Multi-DG Interactions

The voltage variation problem (rise or drop) is a main issue for DG capacity assessment in distribution networks. Typically, rural areas experience voltage rise, while long feeder in urban areas suffer from voltage drop. In contrast, load-center areas are seen as the most cost-efficient locations for maximum DG capacity, maximum loss reduction with minimum impacts on voltage rise and voltage drop. Fig. 1 shows a simple network that contains an OLTC connecting the grid supply point (GSP)

This article has been accepted for inclusion in a future issue of this journal. Content is final as presented, with the exception of pagination.

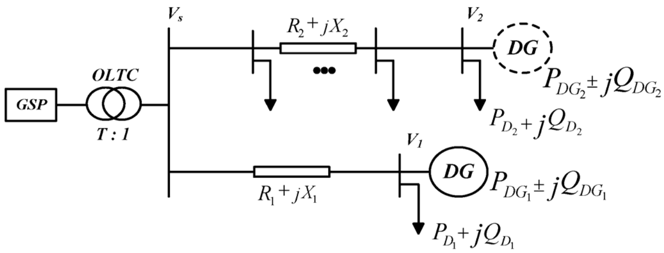

Fig. 1. Simple network system with two DG locations.

to two distribution lines (feeders), and two DG units at bus 1 and bus 2, with local demands.

A. Voltage Rise and DG Capacity

The voltage rise $(\Delta \mathrm{V}^1)$ across the feeder of bus 1 is related to DG active and reactive power injections, load powers, bus 1 voltage (V_1) and secondary voltage (V_s) as expressed in (1):

$$\Delta \mathrm{V}^1 = \mathrm{V}_1 - \mathrm{V}_\mathrm{s} = \frac{\mathrm{R}_1 (\mathrm{P}_{\mathrm{DG}_1} - \mathrm{P}_{\mathrm{D}_1}) + \mathrm{X}_1 (\pm \mathrm{Q}_{\mathrm{DG}_1} - \mathrm{Q}_{\mathrm{D}_1})}{\mathrm{V}_1}. \tag{1}$$

The DG active power can be re-formulated from (1) as described below:

$$\mathrm{P}_{\mathrm{DG}_1} \approx \mathrm{V}_1 \left(\frac{\mathrm{V}_1 - \mathrm{V}_\mathrm{s}}{\mathrm{R}_1} \right) + \left(\frac{\mathrm{R}_1 \mathrm{P}_{\mathrm{D}_1} - \mathrm{X} \mathrm{Q}_{\mathrm{D}_1}}{\mathrm{R}_1} \right) - \left(\frac{\pm \mathrm{X}_1 \mathrm{Q}_{\mathrm{DG}_1}}{\mathrm{R}_1} \right). \tag{2}$$

B. Maximum DG Capacity—Single DG Location

The DG capacity is analyzed considering the unity power factor operation with no load connected to bus 1. Therefore, the maximum DG active power at bus 1 under passive network $(\mathrm{P}_{\mathrm{DG1}}^{\max \mathrm{I}})$ and ANM $(\mathrm{P}_{\mathrm{DG1}}^{\max \mathrm{II}})$ can be approximated from (2) as follows:

$$\mathrm{P}_{\mathrm{DG}_1}^{\max \mathrm{I}} \approx \mathrm{V}_1^{\max} \left(\frac{\mathrm{V}_1^{\max} - \mathrm{V}_\mathrm{s}^{\mathrm{I}}}{\mathrm{R}_1} \right) = \mathrm{V}_1^{\max} \left(\frac{\mathrm{V}_1^{\max} - \mathrm{V}_\mathrm{s}^{\min}}{\mathrm{R}_1} \right) \tag{3}$$

$$\mathrm{P}_{\mathrm{DG}_1}^{\max \mathrm{II}} \approx \mathrm{V}_1^{\max} \left(\frac{\mathrm{V}_1^{\max} - \mathrm{V}_\mathrm{s}^{\mathrm{II}}}{\mathrm{R}_1} \right) \tag{4}$$

where $\mathrm{V}_\mathrm{s}^{\mathrm{I}}$ and $\mathrm{V}_\mathrm{s}^{\mathrm{II}}$ are OLTC secondary voltages under passive networks and ANM, respectively.

In passive network, OLTC is typically utilized to maintain the secondary voltage $(\mathrm{V}_\mathrm{s}^{\mathrm{I}} = \mathrm{V}_\mathrm{s}^{\min})$ at a certain level that ensures the voltage drop along the feeders are within the specified voltage limits, $(\mathrm{V}_2 \geq \mathrm{V}^{\min})$. Under ANM, OLTCs are allowed to control the secondary voltage to maximize the DG capacity, $(\mathrm{V}^{\max} \geq \mathrm{V}_\mathrm{s}^{\mathrm{II}} \geq \mathrm{V}^{\min})$. However, an additional DG capacity can be gained under ANM if the new secondary voltage $(\mathrm{V}_\mathrm{s}^{\mathrm{II}})$ is less than the pre-defined secondary voltage $(\mathrm{V}_\mathrm{s}^{\mathrm{I}})$ under passive network. When no DG is connected at bus 2, the minimum secondary voltage $(\mathrm{V}_\mathrm{s}^{\min})$ to keep the feeder voltage (V_2) within the limit can be depicted in (5):

$$\mathrm{V}_\mathrm{s}^{\min} \geq \mathrm{V}_2^{\min} + \Delta \mathrm{V}_{\mathrm{s}2} \tag{5}$$

where $\Delta \mathrm{V}_{\mathrm{s}2}$ is the voltage drop along the feeder connecting the OLTC and bus 2.

C. Passive Network Management—Multiple DGs

The restriction on the secondary voltage (V_s) could be a limiting factor when studying the effects of multiple DGs (at bus 1 and bus 2) under passive network. From (3), as long as V_s is fixed, no additional DG capacity at bus 1 could be gained by having another DG at different feeder (bus 2).

D. Active Network Management—Multiple DGs

The DG capacity for single DG at bus 1 under ANM in (4) could be affected by introducing other DGs at different locations. The minimum (optimal) value of the secondary voltage $(\mathrm{V}_\mathrm{s}^{\min})$ is directly related to the maximum voltage drop at bus 2, especially during maximum demand and generation case, as in (5). However, if another DG is deployed at bus 2, it could change several factors, such as, reducing the voltage drop along the feeder, reducing power losses and increasing the voltage profile at bus 2. Therefore, the value of the secondary voltage could be reduced further as long as the voltage drop is within the limit. Accordingly, due to the impact of the new added DG at bus 2, the DG capacity at bus 1 in (4) could increase by the additional reduction of the secondary voltage (V_s), as approximated in (6):

$$\left(\mathrm{P}_{\mathrm{DG}_1}^{\max^{\mathrm{II}}} \right)_{\mathrm{new}} = \frac{\mathrm{V}_1^{\max} - \left(\mathrm{V}_\mathrm{s}^{\mathrm{II}} \right)_{\mathrm{new}}}{\mathrm{R}_1} \geq \mathrm{P}_{\mathrm{DG}_1}^{\max^{\mathrm{II}}} \geq \mathrm{P}_{\mathrm{DG}_1}^{\max^{\mathrm{I}}}. \tag{6}$$

It is worth noting that, in passive networks, the multi-DG interaction is limited by the fixed-value of the secondary voltage (V_S) and the DGs locations. On the contrary, as more DGs are deployed under ANM, the multi-DG interaction could lead to changes in the network voltage profile and hence, critically impact (decrease or increase) the DG capacity at certain DG locations. Consequently, planning under certain ANM schemes for specific DG penetration target can also be affected with the increase in DG deployments. For instance, under one ANM scheme (e.g., CVC), the DG capacity can be maximized in the long term with the proper DG allocation and sizing. Hence, extra and costly ANM schemes can be avoided or utilized with lower ratings (e.g., lower energy curtailment's limit, compensator's rating and OLTC's loading).

The aforementioned facts raise the need to consider the impact of multiple DG interactions either for the existing DGs or the future DG deployments. Therefore, in this paper, the multi-configuration multi-period OPF-based technique (MMOPF) is proposed to cater for the multiple DG interaction through incorporating multi-DG configurations and multi-period scenarios.

III. Proposed Multi-Configuration Multi-Period OPF-Based Technique (MMOPF)

The analysis in the previous section illustrates how the DG capacity at certain locations can be affected by the operational status of other DG units. This is the base for the proposed MMOPF which aims: 1) to evaluate and analyze the effects of various multi-DG configurations and multi-period scenarios in a certain distribution network, and 2) to obtain optimal DG capacity for each location that is not affected by the operation of other DGs in the system and can contribute to maximize total DG penetration in the long term.

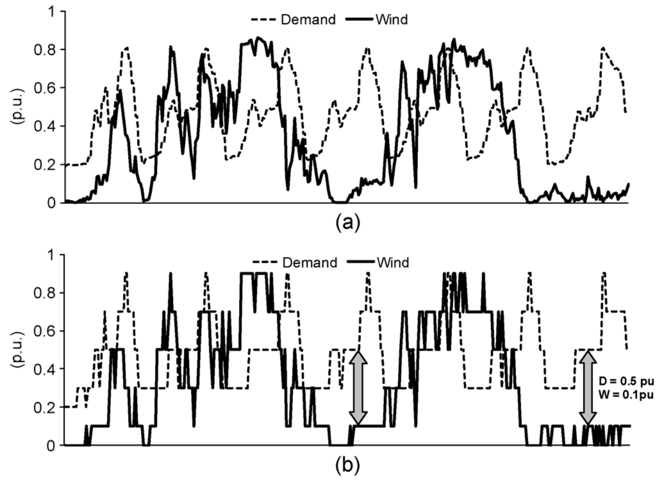

Fig. 2. UKGDS half-hourly domestic economy-demand and renewable wind generation profiles in 2005: 1st week of July [46]. (a) Original profiles. (b) Profiles after the discretization process (before data clustering).

% of Wind Generation \ % of Peak Demand	20	30	50	70	90	100
0	17.5	587.5	729	401.5	241	48
10	32	806	951.5	513.5	233.5	20.5
30	22.5	458	583	320.5	165	18
50	15.5	334	453	280	159.5	24
70	7	240	311	174.5	109	23.5
90	2.5	126	187	103	48	8.5
100	0	1	2	1	1	0.5

Fig. 3. Coincident hours for profile data of demand and wind generation after clustering (aggregation) process.

A. Multi-Period Scenarios: Profiles of Variable Demand and Renewable Generation

In this study, the variability of demand and generation profiles is taken into consideration using historic data for the UK Generic Distribution System (UKGDS), based on half-hourly figures over a one year period (17 520 $\times$ 0.5 h) [46]. A snapshot sample of demand versus wind generation profiles for a one week period is shown in Fig. 2(a), represented by per-unit values (relative to peak).

The original data in [46] is firstly discretized, as shown in Fig. 2(b), and then its similar system-periods are clustered (aggregated) to reduce the total number of periods, based on the method reported in [16]. Fig. 3 illustrates the coincident hours of all multi-period scenarios after the data discretization and clustering processes, in which the total number of 17 520 periods reduced significantly to only 41 periods.

B. Multi-Configurations: Operational Status of DG Units

The conventional OPF-based techniques deal with single or multi-period scenario(s) of demand and generation, such as single and multi-period OPF techniques reported in [16], [43]–[45]. However, these techniques are performed for only one-system configuration where all DGs operating. To incorporate the multi-DG configurations, the conventional OPF techniques are utilized to realize the proposed MMOPF technique. The formulation of multi-configurations to achieve the proposed MMOPF is described as follows:

1) Number of Multi-DG Configurations: In this study, the MMOPF technique aims to incorporate multi-DG configurations, which are defined as the operational status of DG units, and are selected based on the decisions of distribution system planners. The total number of all possible multi-configurations for any number of DG units can be expressed as follows:

$$1 \leq \mathrm{MC_N} \leq (2^{\mathrm{DG_N}} - 1). \tag{7}$$

In (7), the total number of multi-configurations $(\mathrm{MC_N})$ can also be referred as the number of "multi-DG" configurations. For instance, if a system has four DG units, then there can be up to 15 possible multi-DG configurations for the planners to select. If the planners consider the operational status of only one DG unit out of four, then the total number of possible multi-DG configurations would be up to the number of DG units, $(\mathrm{MC_N} \leq \mathrm{DG_N})$, that is up to four configurations.

2) Operational Status of DG Units: After defining the total number of multi-configurations, an important binary parameter should be defined to represent the operational status of DG units at ith bus $(i \in \mathrm{N})$ for every configuration, $(c \in \mathrm{MC_N})$. The operational status of individual DG unit (β_i^C) and all DG units (β) are depicted in (8) and (9):

$$\beta_i^c = \begin{cases} 1, & \text{if a DG at } i^{th} \text{ bus is operating} \\ 0, & \text{otherwise} \end{cases} \tag{8}$$

$$\beta = \begin{bmatrix} \beta_1^1 & \beta_2^1 & \cdots & \beta_N^1 \\ \beta_1^2 & \beta_2^2 & \cdots & \beta_N^2 \\ \vdots & \vdots & \ddots & \vdots \\ \beta_1^c & \beta_2^c & \cdots & \beta_N^c \end{bmatrix}_{(MC_N \times N)}. \tag{9}$$

By considering only the buses with existing DG units (or candidate buses for new DG units), the matrix β in (9) can be particularly defined and described in terms of number and locations of DG units as in (10):

$$\beta = \begin{bmatrix} \beta_{DG_1}^1 & \beta_{DG_2}^1 & \cdots & \beta_{DG_N}^1 \\ \beta_{DG_1}^2 & \beta_{DG_2}^2 & \cdots & \beta_{DG_N}^2 \\ \vdots & \vdots & \ddots & \vdots \\ \beta_{DG_1}^c & \beta_{DG_2}^c & \cdots & \beta_{DG_N}^c \end{bmatrix}_{(MC_N \times DG_N)}. \tag{10}$$

3) Capacity Constraint of DG Units: In the proposed MMOPF technique, there is a capacity constraint for any DG unit according to its operational status for every configuration and can described as follows:

$$0 \leq P_{DG_i}^c \leq \beta_i^c DG^{max} \tag{11}$$

$$P_{DG_i}^c = \begin{cases} 0 \leq P_{DG_i}^c \leq DG^{max} & \forall \quad \beta_i^c = 1 \\ 0 & \forall \quad \beta_i^c = 0. \end{cases} \tag{12}$$

C. Objective Function and Network Constraints

The objective function is to maximize the total DG capacity in each configuration of the multi-configurations, as described in (13). For instance, the maximum capacity of DG units $(P_{DG_i}^c)$ will be obtained across all the multi-configurations:

$$\text{Max} \sum_{\mathrm{c}\in\mathrm{MC_N}} \sum_{\mathrm{i}\in\mathrm{N}} P^{c}_{DG_i} \tag{13}$$

subject to

1) Nodal Power Balance Equations:

$$P^{c}_{G_{i,m}} + \underbrace{P^{c}_{DG_i}\alpha_m}_{P^{c}_{DG_{i,m}}} = \underbrace{\sum_{j\in N} P^{c}_{i,j,m}}_{P^{c}_{i,m}} + P_{D_i}\gamma_m \tag{14}$$

$$Q^{c}_{G_{i,m}} + \underbrace{P^{c}_{DG_i}\alpha_m tan\theta^{c}_{i,m}}_{Q^{c}_{DG_{i,m}}} = \underbrace{\sum_{j\in N} Q^{c}_{i,j,m}}_{Q^{c}_{i,m}} + Q_{D_i}\gamma_m. \tag{15}$$

2) Active and Reactive Line Power Flow Equations:

$$\begin{aligned} P^{c}_{i,j,m} = &- \left(V^{c}_{i,m}\right)^2 G_{ij} + V^{c}_{i,m} V^{c}_{j,m} (G_{ij} \cos\left(\delta^{c}_{i,m} - \delta^{c}_{j,m}\right) \\ &+ Bij \sin(\delta^{c}_{i,m} - \delta^{c}_{j,m})) \end{aligned} \tag{16}$$

$$\begin{aligned} Q^{c}_{i,j,m} &= \left(V^{c}_{i,m}\right)^2 \left(B_{ij} + \frac{1}{2} bc_{ij}\right) + V^{c}_{i,m} V^{c}_{j,m} \\ &\times (G_{ij} \sin\left(\delta^{c}_{i,m} - \delta^{c}_{j,m}\right) - B_{ij} \cos(\delta^{c}_{i,m} - \delta^{c}_{j,m})). \end{aligned} \tag{17}$$

To obtain the line power flow across transformer branches, the secondary voltages are multiplied by the tap-setting (ratio).

3) Operational Network Constraints, $\forall(m \in M), (c \in MC_N)$:

$$P^{min}_{G} \le P^{c}_{G_{i,m}} \le P^{max}_{G} \quad \forall\,(i \in N) \tag{18}$$

$$Q^{min}_{Gi} \le Q^{c}_{G_{i,m}} \le Q^{max}_{Gi} \quad \forall\,(i \in N) \tag{19}$$

$$V^{min}_{i} \le V^{c}_{i,m} \le V^{max}_{i} \quad \forall\,(i \in N) \tag{20}$$

$$T^{min}_{t} \le T^{c}_{t,m} \le T^{max}_{t} \quad \forall\,(i \in N) \tag{21}$$

$$\theta^{min}_{i} \le \theta^{c}_{i,m} \le \theta^{max}_{i} \quad \forall\,(i \in N) \tag{22}$$

$$\sqrt{\left(P^{c}_{i,j,m}\right)^2 + \left(Q^{c}_{i,j,m}\right)^2} \le S^{max}_{ij} \quad \forall\,(i,j \in N). \tag{23}$$

D. Optimal DG Capacity of All Multi-DG Configurations

After optimizing the objective function (13), the maximum capacity of DG units $(P^{c}_{DG_i})$ for every multi-configuration is used to obtain the optimal capacity of all DG units. This ensures that each DG unit can be operated independently without being affected by the operation of other DG units. The formulation for obtaining the optimal DG capacity of each DG unit is depicted in (24):

$$P^{opt}_{DG_i} = min\left[P^{1}_{DG_i}, P^{2}_{DG_i} \ldots P^{c}_{DG_i}\right]_{c\in\mathrm{MC_N}} \quad \forall \quad \beta^{c}_{i} = 1. \tag{24}$$

Similarly, the total DG capacity of all DG units in the system can be formulated from (24) as described in (25):

$$\begin{aligned} P^{opt}_{DG} &= min\left(\begin{bmatrix} P^{1}_{DG_1}, & P^{2}_{DG_1} & \cdots & P^{c}_{DG_1} \\ \vdots & \vdots & \ddots & \vdots \\ P^{1}_{DG_N}, & P^{2}_{DG_N} & \cdots & P^{c}_{DG_N} \end{bmatrix}_{DG_N\times\mathrm{MC_N}}\right) \\ &= \begin{bmatrix} min\left[P^{1}_{DG_i}, P^{2}_{DG_i} \cdots P^{c}_{DG_i}\right]_{c\in MC_N} \\ \vdots \\ min\left[P^{1}_{DG_N}, P^{2}_{DG_N} \cdots P^{c}_{DG_N}\right]_{c\in MC_N} \end{bmatrix}_{DG_N\times 1} \\ &= \begin{bmatrix} P^{opt}_{DG_1} \\ \vdots \\ P^{opt}_{DG_N} \end{bmatrix}_{DG_N\times 1} \\ &= \sum_{i\in DG_N} P^{opt}_{DG_i}. \end{aligned} \tag{25}$$

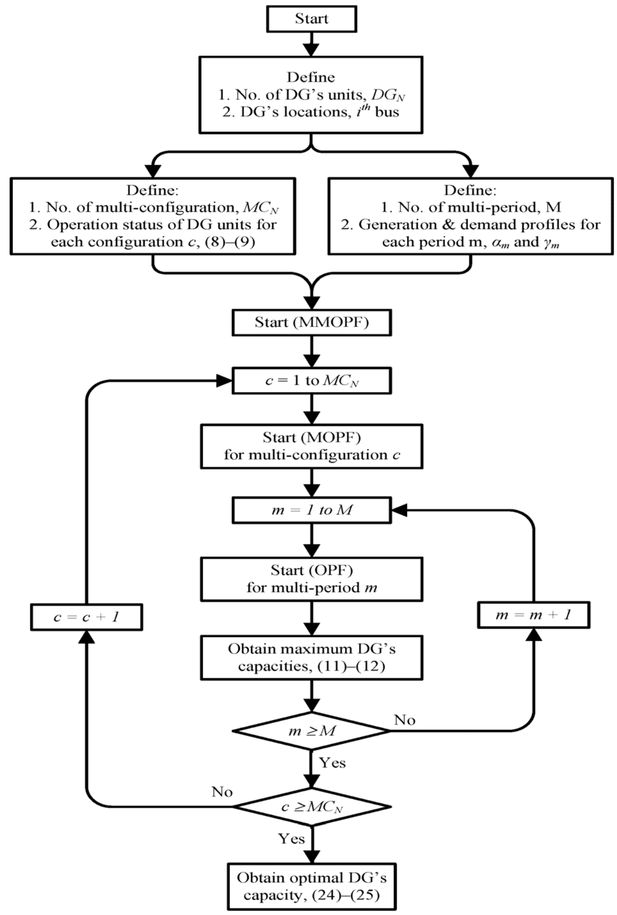

Fig. 4. Flowchart for the proposed MMOPF technique.

E. MMOPF Algorithm

The proposed MMOPF technique firstly solves each configuration of all multi-DG configurations $(c \in MC_N)$ as a subproblem to obtain its maximum DG capacity. The analysis of each configuration also includes multi-period scenarios. After solving each configuration individually, the proposed technique determines the optimal capacity for every DG unit that is applicable for all possible multi-DG configurations. Fig. 4 shows the flowchart of the MMOPF's algorithm.

IV. CAST STUDY

A. Test Network Description

The proposed MMOPF technique is tested on the modified 16-bus 33-kV UK Generic Distribution System

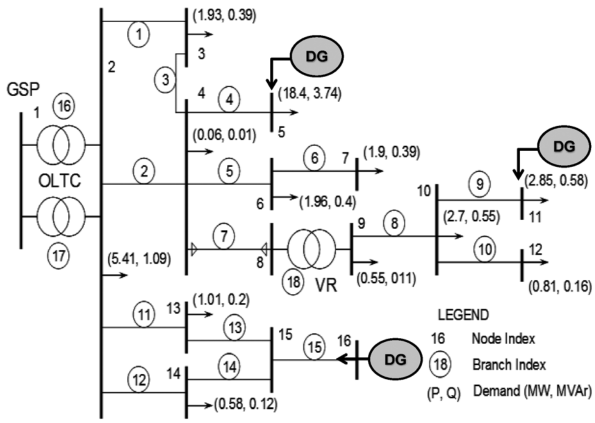

Fig. 5. Modified 16-bus 33-kV UKGDS for MMOPF analysis [46].

(UKGDS)-EHV1 model with the addition of three DG units, as shown in Fig. 5. In this paper, it is assumed that buses 5, 11 and 16 are three possible DG locations but it is noteworthy that the choice of possible DG locations will depend on non-technical factors such as legal requirements, space/land availability and other amenities. These three DG locations represent a load center (at bus 5), a long feeder in urban area (at bus 11) and a rural area (at bus 16). Thus, this selection provides various scenarios of voltage rise and voltage drop, as well as multi-DG interactions under ANM. The thermal line limits at the DG locations are 40 MVA for line 4 (at bus 5) and 15 MVA for both line 9 (at bus 11) and line 15 (at bus 16), respectively. Detailed data of the network parameters can be found in [46]. Based on the 33-kV UK standards [47], the network voltage limits are ±6%, while the power factor of PFC ranges from 0.95 lagging to 0.95 leading. The UKGDS model is implemented in the GAMS software and solved as a nonlinear programming (NLP) problem using the CONOPT solver [48].

B. UK Profiles of Demand and Wind Generation

In this study, the profile data of demand and renewable wind generation for UKGDS is used with half-hourly figures over a one year period [46]. The original profile data that include 17 520 system-periods are discretized and clustered, as described in Section III-A. The two worst-case scenarios of maximum wind generation versus maximum-demand (WCS_1) and minimum-demand (WCS_2) occur at 100% wind generation versus 100% and 30% demand, respectively.

V. Application of the Proposed MMOPF Technique for Planning DG Capacity Under ANM

In this section, the proposed MMOPF technique is tested on the UKGDS network considering four cases studies, as described in Table I. In case studies 1 and 2, the proposed MMOPF is evaluated and compared with the single OPF under WCS_1 and WCS_2, respectively. The variability of demand and wind generation profiles is studied in case studies 3 and 4 using multi-period scenarios, in which the proposed MMOPF technique is compared with the MOPF technique. Case study 4 also investigates the long-term impact of planning certain DG location when only one configuration (single location) is considered instead of multi-configurations (multiple locations), on the total DG penetration in the network.

TABLE I
Case Studies Description: MMOPF Analysis

Case Studies	DG Capacity Limit / Locations			Demand & Generation Scenario	MMOPF Versus
	Bus 5	Bus 11	Bus 16		
1	Max	Max	Max	WCS_1	Single OPF
2	Max	Max	Max	WCS_2	Single OPF
3	Max (Wind)	Max (Wind)	Max (Wind)	Multi-period (m ∈ M)	MOPF
4	Max (Wind)	(10.7MW) (Wind)	Max (Wind)	Multi-period (m ∈ M)	MOPF

TABLE II
Description of Multi-DG Configurations

Multi-Configurations	DG Status / Location		
	Bus 5	Bus 11	Bus 16
1	0	0	1
2	0	1	0
3	0	1	1
4	1	0	0
5	1	0	1
6	1	1	0
7	1	1	1

For all case studies, the DG units are operated at unity power factor and the network is under one ANM scheme (CVC). All the possible multi-DG configurations for the three DG locations are considered using (7), as shown in Table II.

In the conventional OPF/MOPF analysis, the maximum DG capacity is considered under only one configuration of all DG operating (configuration 7, Table II). While, in the proposed MMOPF analysis, the maximum DG capacity for all DG locations $(P^c_{DG_i})$ is firstly evaluated under each configuration $(c \in MC_N)$, and then the optimal DG capacity for all the multi-configurations is obtained for all DG units using (24) and (25).

1) Case Study 1—(WCS_1: Max Demand—Max Generation): Under WCS_1, the maximum DG capacity at bus 16 considering single DG location $(\mathrm{c} = 1)$ is 3.9 MW, which is limited by the voltage rise at bus 16 and the voltage drop at bus 11. This capacity is significantly increased to 7.5 MW and up to 15 MW due to the presence of DGs at buses 5 and 11, individually or together $(\mathrm{c} = 3$, 5 and 7), as given in Table III. However, the maximum DG capacity at bus 5 and bus 11 are not sensitive for all multi-configurations of case study 1, with almost 58.2 MW and 14.2 MW capacities, respectively. The network voltage profiles of all multi-DG configurations in case study 1 are shown in Fig. 6(a).

An interesting observation can be made from Table III. The conventional planning study relies on only one-time system configuration and does not consider the dynamic nature of power system operation. For instance, the total DG penetration level determined using single OPF analysis (configuration 7 in Table III) is 87.4 MW with maximum DG capacity of 58.2 MW (at bus 5), 14.2 MW (at bus 11) and 15 MW (at bus 16). For the same scenario, the maximum (optimal) DG penetration level using the proposed MMOPF is computed as 76.2 MW

TABLE III
CASE STUDY 1: MAXIMUM DG CAPACITY—UNDER WCS_1

Configuration ($c \in MC_N$)	Bus 5 (MW)	Bus 11 (MW)	Bus 16 (MW)	DG Max (MW)
1			3.9	3.9
2		14.2		14.2
3		14.2	7.5	21.7
4	58.2			58.2
5	58.2		15.0	73.2
6	58.2	14.1		72.3
7 (Single OPF)	58.2	14.2	15.0	87.4
(MMOPF)	58.2	14.1	3.9	76.2

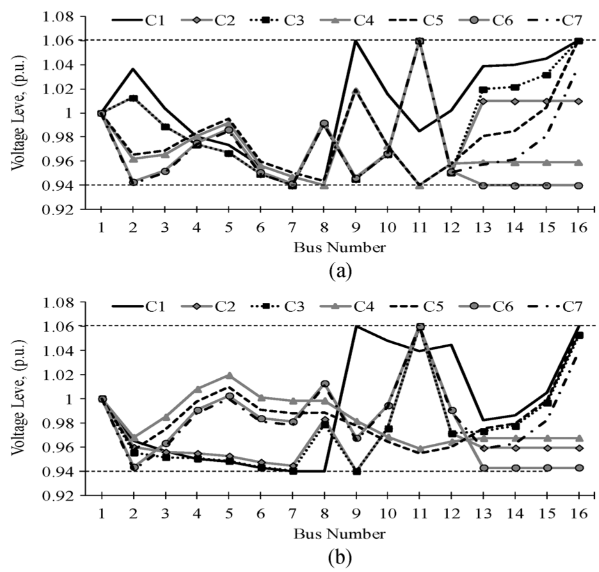

Fig. 6. Voltage profile of all multi-DG configurations. (a): WCS_1, (b): WCS_2.

which is lower than the OPF technique. This is because the optimal DG capacity obtained by OPF analysis is valid for only configuration 7 of all DG operating $(c = 7)$, while, the optimal values obtained by MMOPF analysis are valid for all configurations $(c \in \mathrm{MC_N})$. Further to elaborate, any variability in the system condition, such as, planned or forced outages of DG units, will affect the initially determined DG penetration level. For example, if the DG at bus 5 is not connected to the system, based on the conventional planning study the total DG capacity should reduce to $(87.4\ \mathrm{MW} - 58.2\ \mathrm{MW} = 29.2\ \mathrm{MW})$. However, using the OPF analysis when the DG at bus 5 is not operational, the maximum penetration that can be connected is 21.7 MW (configuration 3 in Table III) with 14.2 MW and 7.5 MW for bus 11 and bus 16, respectively. Subsequently, the DG at bus 16 that is planned with 15 MW has to be switched off due to network constraints (excessive voltage rise), and thus, the total DG capacity will reduce from 21.7 MW to 14.2 MW with only bus 11 connected. This example demonstrates the limitation using OPF-based planning study in which an absence of a DG at certain location may lead to disconnection of another DG(s) in the network.

In contrast, if the DG capacity is planned based on the proposed MMOPF analysis, the presence or absence of a DG at certain location will not affect the DG capacity at other locations. The proposed MMOPF technique determines the DG capacity as 58.2 MW at bus 5, 14.1 MW at bus 11 and 3.9 MW at bus 16 which are optimal values for all possible configurations. If the same aforementioned scenario of switching off the DG at bus 5 is occurs, then the maximum DG penetration using the proposed MMOPF will be 18 MW with 14.1 MW and 3.9 MW at buses 11 and 5. Therefore, with the proposed MMOPF technique, the absence of DG unit at bus 5 will not cause the disconnection for the DG at bus 16 as in the case of single OPF. This case study thus demonstrates the practical applicability and usefulness of the proposed MMOPF technique.

TABLE IV
CASE STUDY 2: MAXIMUM DG CAPACITY-UNDER WCS_2

Configuration ($c \in MC_N$)	Bus 5 (MW)	Bus 11 (MW)	Bus 16 (MW)	DG Max (MW)
1			14.7	14.7
2		10.7		10.7
3		10.7	15.0	25.7
4	45.5			45.5
5	45.5		15.0	60.5
6	45.5	8.5		54.0
7 (Single OPF)	45.5	8.6	15.0	69.1
(MMOPF)	45.5	8.5	14.7	68.7

2) Case Study 2—(WCS_2: Min Demand—Max Generation): The DG penetration levels obtained under WCS_2, for the proposed MMOPF and single OPF techniques are provided in Table IV. The DG capacity at bus 16 is increased significantly to 14.7 MW for single DG configuration (compared to 3.9 MW in case study 1). In contrast, the DG capacity at bus 11 is affected by the voltage rise problem that decreased its capacity from 14.2 MW (case study 1) to 10.7 MW $(c = 2, 3)$, and reduced further to 8.5 MW when a DG at bus 5 is connected $(c = 6, 7)$. The presence of DG at bus 5 has considerable potential (45.5 MW) to maximize the overall DG penetration, although it has impact on reducing the DG capacity at bus 11. Fig. 6(b) illustrates the network voltage profiles for case study 2.

3) Case Study 3—(Multi-Period Scenarios): The impact of variable demand and wind generation profiles is investigated by incorporating the multi-period scenarios that can occur in the network as well as all the seven multi-DG configurations (refer to Fig. 3 and Table II). As illustrated in Table V, the total DG capacity using the proposed MMOPF technique is 57.9 MW (45.5 MW, 8.5 MW and 3.9 MW for bus 5, bus 11 and bus 16, respectively), while, 69.1 MW using the MOPF technique. However, as highlighted previously, the DG capacity obtained using the proposed MMOPF is valid under all the operating conditions. In general, the consideration of multi-DG configurations and multi-period scenarios could result in a better planning for the DG capacity through taking into account various uncertainty and variability associated with the generation of DG units.

4) Case Study 4—(Post-Planning Scenario): Finally, this case study evaluates the impact of a post-planning scenario on the overall planning of DG capacity. It considers planning DG capacity based on only single DG location instead of multiple DG locations. For example, from case study 3, assuming the DG capacity planning is done for only bus 11 which gives 10.7 MW (configuration 2 in Table V). The case study 3 is simulated again

TABLE V
CASE STUDY 3: MAXIMUM DG CAPACITY—MULTI-PERIOD SCENARIOS

Configuration ($c \in MC_N$)	Bus 5 (MW)	Bus 11 (MW)	Bus 16 (MW)	DG Max (MW)
1			3.9	3.9
2		10.7		10.7
3		10.7	7.2	17.9
4	45.5			45.5
5	45.5		13.3	58.8
6	45.5	8.5		54.0
7 (MOPF)	45.5	8.6	15.0	69.1
(MMOPF)	45.5	8.5	3.9	57.9

TABLE VI
CASE STUDY 4: MAXIMUM DG CAPACITY—POST-PLANNING SCENARIO

Configuration ($c \in MC_N$)	Bus 5 (MW)	Bus 11 (MW)	Bus 16 (MW)	DG Max (MW)
1			3.9	3.9
2		10.7 (fixed)		10.7
3		10.7 (fixed)	7.2	17.9
4	45.5			45.5
5	45.5		13.3	58.8
6	8.2	10.7 (fixed)		18.9
7 (MOPF)	8.8	10.7 (fixed)	9.1	28.6
(MMOPF)	8.2	10.7 (fixed)	3.9	22.8

as case study 4 with the post planning of a fixed 10.7 MW at bus 11, based on the "fit-and-forget" approach without considering other DG locations at bus 5 and bus 16.

On this system, if additional DG units are planned to be installed at buses 5 and 16, then the maximum DG capacities that can be achieved are as shown in Table VI. The connection of 10.7 MW at bus 11 critically impacts the DG penetration at bus 5, which is significantly reduced to 8.2 MW ($c = 6$) and 8.8 MW ($c = 7$) compared to 45.5 MW in case study 3. From Tables V and VI, the overall DG capacity is reduced from 57.9 MW to 22.8 MW. This is due to the improper sizing of DG capacity at bus 11 (10.7 MW) during the initial planning stage instead of 8.5 MW as obtained using the proposed MMOPF technique (from Table V).

The constraint of multi-DG configurations in the proposed MMOPF technique, therefore, will be an effective tool for the sizing of DG units that considers and incorporates the analysis of multiple DG locations during the initial planning stage. Furthermore, as discussed in the previous subsections, the sizing of DG units will be independent on the operational status of other DG units. Thus, the network planning based on the proposed MMOPF would certainly contribute to maximize the total DG penetration in the long term.

VI. CONCLUSION

In this paper, a new approach to plan the sizing of DG units, considering the multi-DG configurations, has been proposed. It is illustrated that the multi-DG configurations under ANM schemes could increase or decrease the potential of DG penetration at certain locations. A multi-configuration multi-period OPF technique (MMOPF) has been proposed that allows a better planning to determine the DG capacities at different locations. This technique takes into consideration the impacts of multiple DG interactions by evaluating various uncertainties associated with DG number, locations, size, types and availability. Furthermore, it has been demonstrated that the sizing achieved using the proposed MMOPF technique is independent on the operational status of individual/combined DG units. The proposed technique can be an effective tool for the sizing of DG units at multiple DG locations during the initial planning stage.

REFERENCES

[1] R. C. Dugan, T. E. McDermott, and G. J. Ball, "Planning for distributed generation," *IEEE Ind. App. Mag.*, vol. 7, no. 2, pp. 80–88, Mar./Apr. 2001.
[2] K. Moslehi and R. Kumar, "A reliability perspective of the smart grid," *IEEE Trans. Smart Grid*, vol. 1, no. 1, pp. 57–64, Jun. 2010.
[3] A. Keane *et al.*, "Evaluation of advanced operation and control of distributed wind farms to support efficiency and reliability," *IEEE Trans. Sustain. Energy*, vol. 3, no. 4, pp. 735–742, Oct. 2012.
[4] R. A. Walling, R. Saint, R. C. Dugan, J. Burke, and L. A. Kojovic, "Summary of distributed resources impact on power delivery systems," *IEEE Trans. Power Del.*, vol. 23, no. 3, pp. 1636–1644, Jul. 2008.
[5] P. P. Barker and R. W. De Mello, "Determining the impact of distributed generation on power systems. I. Radial distribution systems," in *Proc. IEEE Power Eng. Soc. Summer Meeting*, 2000, vol. 3.
[6] E. Coster, J. Myrzik, B. Kruimer, and W. Kling, "Integration issues of distributed generation in distribution grids," *Proc. IEEE*, vol. 99, no. 1, pp. 28–39, Jan. 2011.
[7] M. Nagpal, F. Plumptre, R. Fulton, and T. G. Martinich, "Dispersed generation interconnection-utility perspective," *IEEE Trans. Ind. App.*, vol. 42, no. 3, pp. 864–872, May–Jun. 2006.
[8] Z. Liu, F. Wen, and G. Ledwich, "Optimal siting and sizing of distributed generators in distribution systems considering uncertainties," *IEEE Trans. Power Del.*, vol. 26, no. 4, pp. 2541–2551, Oct. 2011.
[9] H. Yu, C. Y. Chung, K. P. Wong, and J. H. Zhang, "A chance constrained transmission network expansion planning method with consideration of load and wind farm uncertainties," *IEEE Trans. Power Syst.*, vol. 24, no. 3, pp. 1568–1576, Aug. 2009.
[10] K. Zou, A. P. Agalgaonkar, K. M. Muttaqi, and S. Perera, "Distribution system planning with incorporating DG reactive capability and system uncertainties," *IEEE Trans. Sustain. Energy*, vol. 3, no. 1, pp. 112–123, Jan. 2012.
[11] A. Soroudi and M. Afrasiab, "Binary PSO-based dynamic multi-objective model for distributed generation planning under uncertainty," *IET Renew. Power Gener.*, vol. 6, no. 2, pp. 67–78, Mar. 2012.
[12] E. Ela and M. O'Malley, "Studying the variability and uncertainty impacts of variable generation at multiple timescales," *IEEE Trans. Power Syst.*, vol. 27, no. 3, pp. 1324–1333, Aug. 2012.
[13] V. Hamidi, F. Li, and L. Yao, "Value of wind power at different locations in the grid," *IEEE Power Del.*, vol. 26, no. 2, pp. 526–537, Apr. 2011.
[14] P. Djapic, C. Ramsay, D. Pudjianto, G. Strbac, J. Mutale, N. Jenkins, and R. Allan, "Taking an active approach," *IEEE Power Energy Mag.*, vol. 5, no. 4, pp. 68–77, Jul.–Aug. 2007.
[15] S. N. Liew and G. Strbac, "Maximising penetration of wind generation in existing distribution networks," *IEE Gener. Transm. Distrib.*, vol. 149, no. 3, pp. 256–262, May 2002.
[16] L. F. Ochoa, C. J. Dent, and G. P. Harrison, "Distribution network capacity assessment: Variable DG and active networks," *IEEE Trans. Power Syst.*, vol. 25, no. 1, pp. 87–95, Feb. 2010.
[17] P. Siano, P. Chen, Z. Chen, and A. Piccolo, "Evaluating maximum wind energy exploitation in active distribution networks," *IET Gener. Transm. Distrib.*, vol. 4, no. 5, pp. 598–608, 2010.
[18] L. F. Ochoa and G. P. Harrison, "Minimizing energy losses: Optimal accommodation and smart operation of renewable distributed generation," *IEEE Trans. Power Syst.*, vol. 26, no. 1, pp. 198–205, Feb. 2011.
[19] R. Tonkoski, L. A. C. Lopes, and T. H. M. El-Fouly, "Coordinated active power curtailment of grid connected PV inverters for overvoltage prevention," *IEEE Trans. Sustain. Energy*, vol. 2, no. 2, pp. 139–147, Apr. 2011.
[20] Q. Zhou and J. W. Bialek, "Generation curtailment to manage voltage constraints in distribution networks," *IET Gener. Transm. Distrib.*, vol. 1, no. 3, pp. 492–498, May 2007.
[21] S. C. E. Jupe, P. C. Taylor, and A. Michiorri, "Coordinated output control of multiple distributed generation schemes," *IET Renew. Power Gener.*, vol. 4, no. 3, pp. 283–297, May 2010.

[22] A. Keane, Q. Zhou, J. W. Bialek, and M. O'Malley, "Planning and operating non-firm distributed generation," *IET Renew. Power Gener.*, vol. 3, no. 4, pp. 455–464, Dec. 2009.

[23] T. Boehme, G. P. Harrison, and A. R. Wallace, "Assessment of distribution network limits for non-firm connection of renewable generation," *IET Renew. Power Gener.*, vol. 4, no. 1, pp. 64–74, Jan. 2010.

[24] R. A. F. Currie, G. W. Ault, and J. R. McDonald, "Methodology for the determination of the economic connection capacity for renewable generator connections to distribution networks optimised by active power flow management," *Proc. Inst. Elect. Eng., Gener., Transm. Distrib.*, vol. 153, no. 4, pp. 456–462, Jul. 2006.

[25] R. A. F. Currie, G. W. Ault, R. W. Fordyce, D. F. MacLeman, M. Smith, and J. R. McDonald, "Actively managing wind farm power output," *IEEE Trans. Power Syst.*, vol. 23, no. 3, pp. 1523–1524, Aug. 2008.

[26] O. Samuelsson, S. Repo, R. Jessler, J. Aho, M. Karenlampi, and A. Malmquist, "Active distribution network—Demonstration project ADINE," in *Proc. IEEE PES Innovative Smart Grid Technologies Conf. Europe (ISGT Europe)*, Oct. 2010.

[27] G. Strbac, C. Ramsay, and D. Pudjianto, "Integration of distributed generation into the UK power system," in *DTI Centre for Distributed Generation and Sustainable Electrical Energy*. London, U.K.: Imperial College London, Mar. 2007.

[28] M. J. Dolan *et al.*, "Distribution power flow management utilizing an online optimal power flow technique," *IEEE Trans. Power Syst.*, vol. 27, no. 2, pp. 790–799, May 2012.

[29] F. Pilo, G. Pisano, and G. G. Soma, "Optimal coordination of energy resources with a two-stage online active management," *IEEE Trans. Ind. Electron.*, vol. 58, no. 10, pp. 4526–4537, Oct. 2011.

[30] C. Cecati, C. Citro, and P. Siano, "Combined operations of renewable energy systems and responsive demand in a smart grid," *IEEE Trans. Sustain. Energy*, vol. 2, no. 2, pp. 468–476, Oct. 2011.

[31] S. L. Hay, G. W. Ault, K. R. W. Bell, and J. R. McDonald, "System operator interfaces to active network management schemes in future distribution networks," in *Proc. 43rd Int. Universities Power Eng. Conf. (UPEC)*, Sep. 2008.

[32] D. Papadaskalopoulos, E. Manitsas, P. Mancarella, and G. Strbac, "Optimization of operating and investment costs of active management deployment in distribution networks," in *IEEE Trondheim PowerTech*, Jun. 2011.

[33] A. Shafiu, T. Bopp, I. Chilvers, and G. Strbac, "Active management and protection of distribution networks with distributed generation," in *Proc. IEEE Power Eng. Soc. General Meeting*, Jun. 2004.

[34] R. Hidalgo, C. Abbey, and G. Joos, "Technical and economic assessment of active distribution network technologies," in *Proc. IEEE Power Energy Soc. General Meeting*, Jul. 2011.

[35] Z. Hu and F. Li, "Cost-benefit analyses of active distribution network management, part I: Annual benefit analysis," *IEEE Trans. Smart Grid*, vol. 3, no. 3, pp. 1067–1074, Sep. 2012.

[36] C. L. Masters, "Voltage rise: The big issue when connecting embedded generation to long 11 kV overhead lines," *Power Eng. J.*, vol. 16, no. 1, pp. 5–12, Feb. 2002.

[37] P.-C. Chen *et al.*, "Analysis of voltage profile problems due to the penetration of distributed generation in low-voltage secondary distribution networks," *IEEE Trans. Power Del.*, vol. 27, no. 4, pp. 2020–2028, Oct. 2012.

[38] C. Dent, L. F. Ochoa, and G. P. Harrison, "Network distributed generation capacity analysis using OPF with voltage step constraints," *IEEE Trans. Power Syst.*, vol. 25, no. 1, pp. 296–304, Feb. 2010.

[39] H. M. Ayres, W. Freitas, M. C. De Almeida, and L. C. P. Da Silva, "Method for determining the maximum allowable penetration level of distributed generation without steady-state voltage violations," *IET Gener. Transm. Distrib.*, vol. 4, no. 4, pp. 495–508, 2010.

[40] A. Keane and M. O'Malley, "Optimal allocation of embedded generation on distribution networks," *IEEE Trans. Power Syst.*, vol. 20, no. 3, pp. 1640–1646, Aug. 2005.

[41] A. A. Tamimi, A. Pahwa, and S. Starrett, "Effective wind farm sizing method for weak power systems using critical modes of voltage instability," *IEEE Trans. Power Syst.*, vol. 27, no. 3, pp. 1610–1617, Aug. 2012.

[42] D. J. Burke and M. J. O'Malley, "Maximizing firm wind connection to security constrained transmission networks," *IEEE Trans. Power Syst.*, vol. 25, no. 2, pp. 749–759, May 2010.

[43] R. P. Payasi1, A. K. Singh, and D. Singh, "Review of distributed generation planning: Objectives, constraints, and algorithms," *Int. J. Eng., Sci., Technol.,* MultiCraft Ltd., vol. 3, no. 3, pp. 133–153, 2011.

[44] A. Keane, L. F. Ochoa, C. L. T. Borges, G. W. Ault, A. D. Alarcon-Rodriguez, R. A. F. Currie, F. Pilo, C. Dent, and G. P. Harrison, "State-of-the-art techniques and challenges ahead for distributed generation planning and optimization," *IEEE Trans. Power Syst.*, to be published.

[45] P. S. Georgilakis and N. D. Hatziargyriou, "Optimal distributed generation placement in power distribution networks: Models, methods, and future research," *IEEE Trans. Power Syst.*, to be published.

[46] Distributed Generation and Sustainable Electrical Energy Centre. United Kingdom Generic Distribution System (UKGDS). [Online]. Available: http://www.sedg.ac.uk.

[47] M. Tsili and S. Papathanassiou, "A review of grid code technical requirements for wind farms," *IET Renew. Power Gener.*, vol. 3, no. 3, pp. 308–332, Sep. 2009.

[48] General Algebraic Modeling System (GAMS), GAMS—A User's Guide, 2012. [Online]. Available: http://www.gams.com/.

Sultan S. Al Kaabi (S'07–M'09) received the B.Sc. degree in electrical engineering from UAE University, Al Ain, UAE, in 2009, and the M.Sc. degree in electrical power engineering from Masdar Institute of Science & Technology, Abu Dhabi, UAE, in 2013, where he is currently pursuing the Ph.D. degree in electrical power engineering.

Since 2009, he has been working for Abu Dhabi Water & Electricity Authority (ADWEA) in Al Ain Distribution Company (AADC), Al Ain, UAE. His current research interests include power systems analysis, planning and optimization of distributed generations, and active network management.

Mr. Al Kaabi is a member of GCC-Cigre Study Committee no. 5, titled: "System Performance Development and Renewable Energy".

H. H. Zeineldin (M'06–SM'13) received the B.Sc. and M.Sc. degrees in electrical engineering from Cairo University, Egypt, in 1999 and 2002, respectively. In 2006, he received the Ph.D. degree in electrical and computer engineering from the University of Waterloo, Waterloo, ON, Canada.

He worked for Smith and Andersen Electrical Engineering Inc. where he was involved with projects involving distribution system design, protection and distributed generation. He then worked as a Visiting Professor at the Massachusetts Institute of Technology (MIT), Cambridge, MA, USA. Currently, he is an associate professor with the Masdar Institute of Science and Technology in Abu Dhabi, UAE and previously, a faculty member in the Faculty of Engineering at Cairo University in Egypt. His current interests include power system protection, distributed generation, and micro-grids.

Vinod Khadkikar (S'06–M'09) received the B.E. degree from the Government College of Engineering, Dr. Babasaheb Ambedkar Marathwada University, Aurangabad, India, in 2000, the M.Tech. degree from the Indian Institute of Technology (IITD), New Delhi, India, in 2002, and the Ph.D. degree from the École de Technologie Supérieure (E.T.S.), Montréal, QC, Canada, in 2008, all in electrical engineering.

From December 2008 to March 2010, he was a Postdoctoral Fellow at the University of Western Ontario, London, ON, Canada. Since April 2010, he has been an Assistant Professor at Masdar Institute of Science and Technology, Abu Dhabi, UAE. From April 2010 to December 2010, he was a visiting faculty at Massachusetts Institute of Technology, Cambridge, MA, USA. His research interests include applications of power electronics in distribution systems and renewable energy resources, grid interconnection issues, power quality enhancement, active power filters and electric vehicles.